Available online at www.sciencedirect.com
ScienceDirect
Journal of the European Ceramic Society 32 (2012) 1383–1387
www.elsevier.com/locate/jeurceramsoc

The effect of Al–O substitution for Si–N on the luminescence properties of YAG:Ce phosphor

Małgorzata Sopicka-Lizer[a], Daniel Michalik[a,*], Julian Plewa[b], Thomas Juestel[b], Holger Winkler[c], Tomasz Pawlik[a]

[a] *Silesian University of Technology, 40-019 Katowice ul. Krasińskiego 8, Poland*
[b] *University of Applied Science Muenster, 48565 Steinfurt, Stegerwaldstr. 39, Germany*
[c] *MERCK KGaA, 64293 Darmstadt, Frankfurter Strasse 250, Germany*

Available online 13 May 2011

Abstract

The present paper describes the effect of various Si–N substitution degree on the crystal structure and optical properties of yellow YAG:Ce phosphor commonly used with combination of InGaN in white LEDs. It has been found that the course of silicon/nitrogen YAG:Ce garnet doping as well as formation of the liquid phase and its chemical composition controlled formation of the side phase besides YAG:Ce. Substitution of Al–O for Si–N chemical bonds according to the general formula $Y_{2.94}Ce_{0.06}Al_{(5-x)}Si_xO_{(12-x)}N_x$ was confirmed by changes of the unit cell parameter and formation of the Si–N bonds as detected by FT-IR studies. Formation of the nitrogen ligand in cerium arrangement resulted in a red shift in emission spectrum of trivalent cerium if nominal x value was in the range of 0.2–0.3. Above $x = 0.3$ only decrease of emission intensity was observed because of the secondary phase precipitation but further solution of Si–N in YAG:Ce crystal lattice cannot be excluded.

Keywords: Powders-solid state reaction; Optical properties; Si_3N_4; YAG:Ce

1. Introduction

Light emitting diodes (LEDs) are the most developing branch of the energy-saving light sources because of low energy consumption, high reliability, long life, lightweight, absence of mercury and a small size. Cerium doped yttrium aluminium garnet (YAG:Ce) is a commonly applied yellow phosphor powder combining the yellow emission with blue InGaN LED for giving white LED light with a cool white colour temperature (CCT) over 4500 K. However, application of white LEDs in general lightening requires decrease of the colour temperature and it could be done if a red-shift of Ce^{3+} emission was accomplished.[1] The change of the emission wavelength of trivalent cerium would be possible if the energy position of the lowest Ce^{3+} $5d^1$ level was modified by the covalency and polarizability of Ce^{3+}–ligand bonds.[2] Incorporation of nitrogen N^{3-} into the nearest coordination sphere of cerium and formation of Ce–N bonds instead of oxygen bonded activator ion will result in lower electronegativity difference and would lower the energy of the $5d^1$ levels. There are reports that incorporation of silicon in the form of Si_3N_4 into $(Sr,Ba,Ca)Al_{2-x}Si_xO_{4-x}N_x:Eu^{2+}$ [3] or addition of Si_2N_2O[4] or Si_3N_4 into YAG[5] resulted in the redshift of the emission.

YAG is a complex crystal structure with two of Al^{3+} ions situated in octahedral positions and three remaining Al^{3+} ions are in tetrahedral sites while cerium activator occupies dodecahedral yttrium position. Similarity of Al–O (1.761 Å) and Si–O (1.7535 Å) bond lengths in tetrahedral coordination as well as the same charge difference between cation and anion (−1) offers large extent of solubility as it occurs in SiAlONs.[6] However, the efficient nitrogen substitution in the YAG structure could occur only if $[AlO_4]^{5-}$ tetrahedra are replaced by $[SiN_4]^{8-}$. On the other hand, the charge balance requires simultaneous incorporation of the relevant cation or substitution of one $[AlO_4]^{5-}$ tetrahedra for $[SiN_4]^{8-}$ would have to be accompanied by the subsequent incorporation of the three $[SiO_4]^{4-}$. Thus substitution of $[AlO_4]^{5-}$ for $[SiO_3N]^{5-}$ seems to be the most favourable and opens the solubility limit of nitrogen up to 3.75 at.% in YAG:Ce while the reported values are well below that value.[4,5,7] The present paper describes the effects of Si–N solubility in

* Corresponding author.
E-mail addresses: malgorzata.sopicka-lizer@polsl.pl (M. Sopicka-Lizer), daniel.michalik@polsl.pl (D. Michalik), plewa@fh-muenster.de (J. Plewa), tj@fh-muenster.de (T. Juestel), holger.winkler@merck.de (H. Winkler), tomasz.pawlik@polsl.pl (T. Pawlik).

0955-2219/$ – see front matter © 2011 Elsevier Ltd. All rights reserved.
doi:10.1016/j.jeurceramsoc.2011.04.021

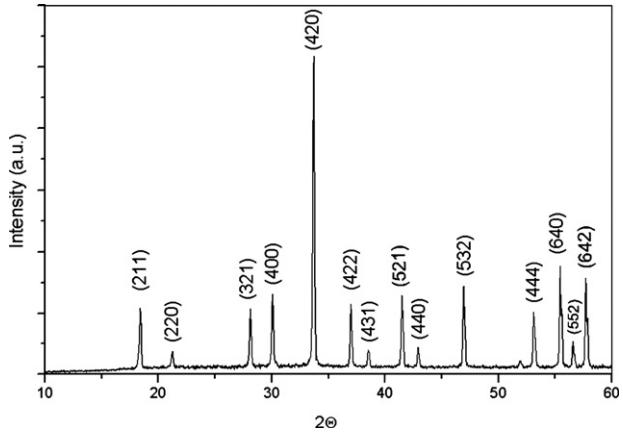

Fig. 1. XRD pattern of the 0.25-H specimen after synthesis at 1650 °C.

the YAG:Ce structure as measured by structural and optical methods.

2. Experimental methods

The samples with the general formula of $Y_{3-a}Ce_aAl_{(5-x)}Si_xO_{(12-x)}N_x$ ($a = 0.06$; $x = 0$–0.6) were manufactured by a conventional solid-state reaction. One reference YAG sample without cerium oxide ($a = 0$) was prepared by the same method as a reference material. The stoichiometric amount of raw powders Y_2O_3 (Treibacher, 99.99%), α-Al_2O_3 (Alfa Aesar, 99.99%), α-Si_3N_4 (UBE, >98%), CeO_2 (AtomicChemetals, 99.99%) as a luminescence activator were batched as the based materials. 1 wt% of AlF_3 (Aldrich, 99.9%) was added to the mixture as a flux typically used in YAG:Ce manufacturing and 1.6 excess of Si_3N_4 was used in order to compensate silicon evaporation. Estimation of silicon nitride excess was based on thermodynamical prediction.[8] The batched powders were mixed on a roller bench with Si_3N_4 milling bodies in MEK/ET solvent with addition of a surfactant (hypermer KD1, Uniqema). The suspension was then evaporated and dried for 2 hours at 120 °C. Calcination was performed in a tube furnace for 8 h in N_2/H_2 gas-flow at 1650 °C.

A Rigaku MiniFlex II diffractometer was used for taking the powder diffraction patterns. They were collected in the 2θ range of 10–60° with a step size of 0.02° using Cu $K\alpha_1$ radiation with $\lambda = 1.54053$ nm with nickel filter. A variety of scanning speeds were tried: 0.1, 1.0 and 10° per minute (Fig. 1). The structure refinement was performed by Rietveld method using the Maud software. It has been found that scanning speed of 1.0° per minute was satisfactory and phase composition of the resultant samples as well as unit cell parameters were calculated with accuracy ±0.0005 Å. Estimation of the YAG:Ce unit cell parameter change due to the Al–O substitution for Si–N was done assuming proportional changes of the unit cell length if x amount of Al–O bonds (1.761 Å) was replaced by Si–N bonds (1.7535 Å). Equilibrium phase composition at 1650 °C was calculated[8] for each oxide with silicon nitride separately considering the effect of atmosphere and flux.

Table 1
Phase assemblage of the specimens with the nominal composition of $Y_{2.94}Ce_{0.06}Al_{(5-x)}Si_xO_{(12-x)}N_x$.

No.	x + constant 1.6 excess of Si_3N_4	Phases
	0.0	100% YAG
0.1-H	0.1	100% YAG
0.2-H	0.2	100% YAG
0.25-H	0.25	100% YAG
0.3-H	0.3	97.8% YAG, 2.2% $Y_2Si_3O_3N_4$
0.4-H	0.4	97.5% YAG, 2.5% $Y_2Si_3O_3N_4$
0.5-H	0.5	96.8% YAG, 3.2% $Y_2Si_3O_3N_4$
0.6-H	0.6	96.3% YAG, 3.7% $Y_2Si_3O_3N_4$

Excitation and emission spectra were measured with an Edinburgh Instruments FS900 spectrometer equipped with 450 W Xe arc lamp, mirror optics for powder samples and cooled single photon counting photomultiplier (Hamamatsu R2658). Excitation and emission spectra were recorded in the regions of 250–550 nm and 460–800 nm respectively. Reflection spectra were recorded on ARC SpectraPro-300i (Acton Research Corporation) spectrometer equipped with 450 W Xe arc lamp, single photon counting photomultiplier and integration sphere. Reflection spectra were recorded in the region of 250–800 nm with the steps of 1 nm. Barium sulphate ($BaSO_4$, 99.998% purity, Alfa Aesar, Germany) was used as a white standard. All measurements were carried out at room temperature. FTIR spectroscopy (Model FTS-60v, Bio-RAD spectrometer) was carried out on the mixture of the initial powders, YAG:Ce without Si,N substitution and powders with the relevant substitution. FTIR studies were recorded in the range of 400–4000 cm^{-1} on samples suspended in KBr pellets in the absorbance mode. Accuracy of the bands shift was ±2 cm^{-1}. Content of nitrogen was measured with Eltra ON-900 oxygen/nitrogen equipment. The resultant powders were observed in SEM (Hitachi 3400N) and TEM (Hitachi HD-2300A).

3. Results and discussion

Si,N doped YAG:Ce samples with the nominal nitrogen substitution in the range of $x = 0.1$–0.6 were synthesised at 1650 °C in a standard solid-state processing with AlF_3 flux addition. Reducing atmosphere of the synthesis was provided by N_2/H_2 flow in a tube furnace. The XRD results showed that monophase YAG was obtained if x in the nominal composition was below 0.3. Further increase of a silicon nitride content in the starting mixture led to precipitation of Si_3N_4 in the form of $Si_3N_4 * Y_2O_3$ (nitrogen melilite) phase and obviously must had changed the stoichiometry of the remaining components for garnet formation (Table 1). Quantity of melilite in the resultant powder increases with growing amount of silicon nitride in the initial mixture thus could be ascribed to the solubility limit. Moreover, the observed limit of Si,N solubility in the YAG:Ce structure is consistent with previous reports showing that nitrogen solubility limit in YAG (x) does not exceed 0.35 if manufactured in N_2/H_2 atmosphere.[5] However, both results show only the nom-

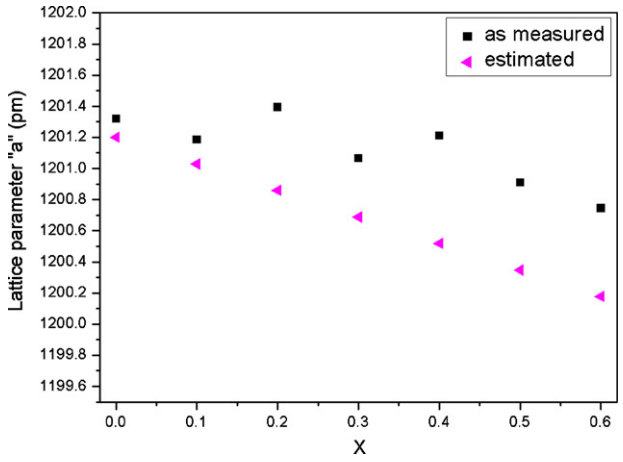

Fig. 2. Measured and estimated cell parameters of $Y_{3-a}Ce_aAl_{(5-x)}Si_xO_{(12-x)}N_x$.

inal value of Si,N substitution and do not consider evaporation of the volatile species and the applied Si_3N_4 excess (by factor 1.6 in the present studies). The measured amount of nitrogen in 0.25-H specimen shows higher nitrogen content (1.4 wt%) in comparison to the expected value of 0.59 wt% or 0.93 wt% if no silicon nitride was lost during the synthesis. Thermodynamic calculation shows that all starting oxides can form nitrides in the reducing atmosphere at 1650 °C. Besides the measured value of nitrogen amount does not confirm yet its solubility in the YAG structure since non-detected nitrogen-bearing amorphous phase can be present in the tested specimens. This shows that the true solubility of Si and N is only roughly estimated.

The other possibility to evidence the YAG:Ce crystal lattice modification is presented in Fig. 2 as a relationship between the lattice parameter and a nominal Si,N substitution in $Y_{2.94}Ce_{0.06}Al_{(5-x)}Si_xO_{(12-x)}N_x$ specimens. Substitution of larger Ce^{3+} ions (128.3 pm) for dodecahedral Y^{3+} ions (115.9 pm) leads to growth of the YAG unit cell parameter till 1201.32 pm as measured in the present work or presented elsewhere: 1201.2 pm if $a = 0.06$.[1] The last value was used to estimate changes of the unit cell parameters due to Al,O substitution for Si,N if Al–O bond of 176.1 pm length in tetrahedral sites is replaced by slightly shorter (175.35 pm) Si–N bonds. The estimated trend of the unit cell contraction due to the formation of solid solution is in a good agreement with the measured values, apart from the nominal values of the substitution degree. It should be noted, however, that decrease of the Si,N doped YAG:Ce unit cell continues regardless the melilite precipitation. Moreover, changes of the crystal lattice deviate from the calculated trend over $x = 0.2$ thus formation of melilite could occur at lower amount of silicon nitride but its amount is too low to be detected by XRD as a separate crystalline phase. It means that incorporation of silicon and nitrogen into the YAG crystal lattice would be possible to the greater extent but melilite occurred. The latter does not form the eutectic liquid with Si_3N_4 and would precipitate if Al–Y–Si–O–N liquid was saturated with nitrogen. Since SEM/TEM studies (Fig. 3) of the calcined powders reveal only the limited sintering of the powder particles thus the amount of liquid must have been restricted and its chemical composition

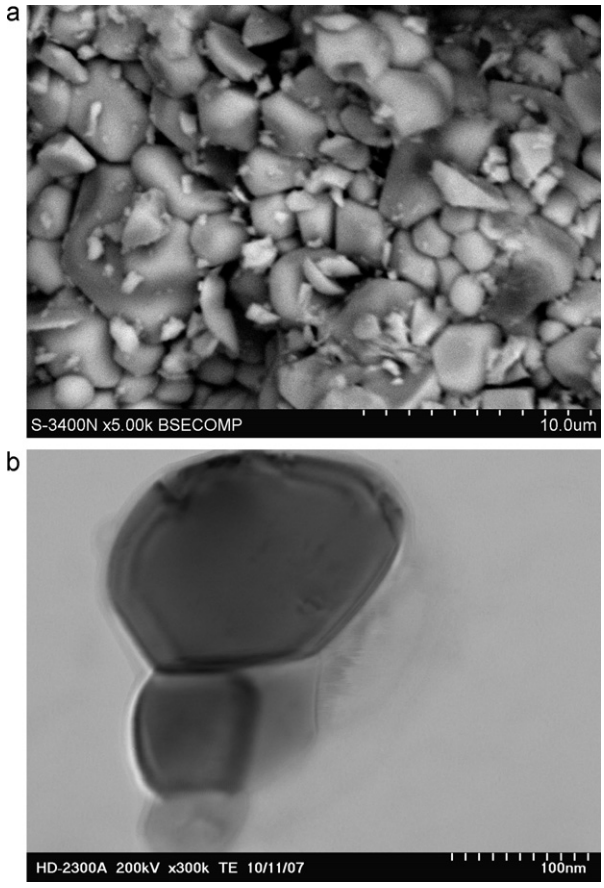

Fig. 3. Morphology of Si,N-doped ($x = 0.3$) YAG:Ce particles after synthesis at 1650 °C; (a) SEM image, (b) TEM image.

controls the course of Si dissolution in the YAG crystal lattice with charge compensation of nitrogen. That finding opens possibilities for technological improvement for extending the solubility limit in YAG:Ce phosphors.

Table 2 lists all IR absorption bands of the initial powders mixture for (Si,N)YAG:Ce as well as synthesized YAG:Ce and

Table 2
Positions of the FTIR absorption bands of the initial powder mixture, YAG:Ce and Si,N doped YAG:Ce compared with the literature data.

Bonds	Wavenumbers (cm^{-1})			Reference
	Starting mixture	YAGr:Ce	(Si,N)YAG:Ce	
Al–O, Si–N	417	–	–	[9,11,12]
AlO_6, Y–O	463	474	466	[11,12]
Si–N	497	–	–	[9]
Al–O	510	515	516	[11,12]
Al–O, Y–O	561	568	570	[11,12]
Al–O	685	696	693	[11,12]
Y–O	734	729	725	[11,12]
Al–O	755	790	790	[11,12]
Si–N	854	–	–	[9]
Si–O	894	–	–	[9]
Si–N	906	–	901	[9]
O–Si–N_3	935	–	949	[9,13]
SiN_4	1037	–	1022	[9,13]
Ce–O	–	1081	1079	[14,15]

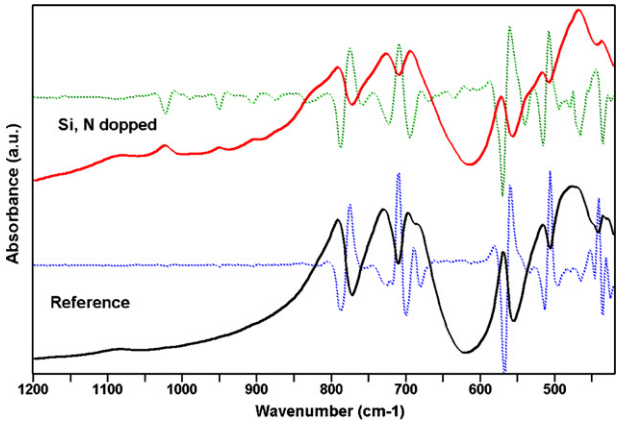

Fig. 4. FT-IR spectra of YAG:Ce samples without doping (reference specimen) and doped with Si–N ($x = 0.3$). The spectra are given by the continuous lines while their derivates are marked by the dotted lines.

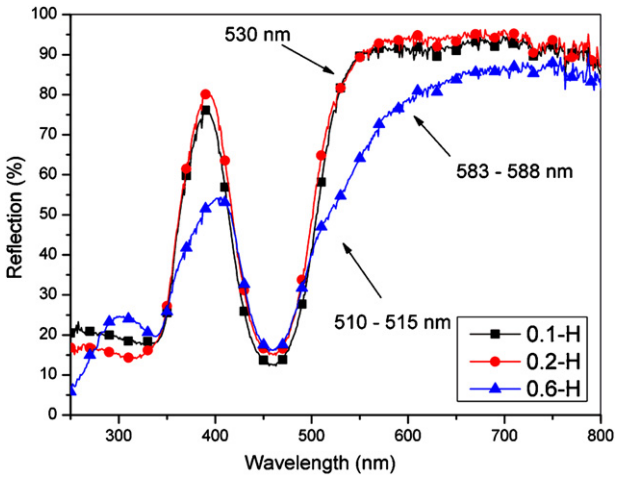

Fig. 5. Reflection spectra of (Si,N) doped YAG:Ce powders with nominal composition of $Y_{2.94}Ce_{0.06}Al_{(5-x)}Si_xO_{(12-x)}N_x$ for $x = 0$–0.6.

doped (Si,N)YAG:Ce compounds. The latter was checked for $x = 0.2$ and $x = 0.3$ but no significant changes between spectra of both specimens were visible. The bands were compared with the literature data and ascribed to the relevant Al–O and Y–O lattice vibration. All the metal–oxygen stretching vibrations are present in the initial mixture but positions of the band are slightly shifted to the higher wavenumber after formation of YAG:Ce compound. Distinctions between nitrogen doped and undoped YAG:Ce specimens are very subtle, in the range of the instrument resolution, if merely Al–O and Y–O vibrations are considered. The only one dissimilarity can be noticed for a position of 463 cm^{-1} band for Y–O vibrations which could be affected by the partial substitution of Si–N bonds in the Y–O–Al bridge. The above mentioned discrepancy is illustrated in Fig. 4 demonstrating IR-spectra and their derivatives of YAG:Ce and Si,N-doped ($x = 0.2$) YAG:Ce powders. Calculated derivatives show more clearly other deformations of Al–O and Y–O bands due to Si,N doping.

The bands related to the vibration of Si–N bonds are visible in the range of 800–1100 cm^{-1} and are easily resolved as they are not present in the undoped YAG:Ce sample (Table 2) as well as can be clearly visible in Fig. 4. The band at 1037 cm^{-1} is typical to vibration of Si–N bonds in SiN_4 tetrahedral and appears at 1034[9] or 1040 cm^{-1} [10] in α-Si_3N_4. It is shifted to smaller wavenumbers in Si,N doped YAG:Ce (1022 cm^{-1}) because of Al–O dominating sites in the YAG lattice. The opposite shift to higher wavenumbers is observed if Si–N bonds in SiN_4 tetrahedral are replaced by Al–O in β-SiAlON.[13]

The remaining band at 1080 cm^{-1} is not ascribed to any vibrating metal–oxygen bond and was not found in the mixture of the initial powders. There were suggestions in the literature that the wavenumber of the anti-symmetric stretching Si–O–Si vibration (1120 cm^{-1}) could be decreased to 1088 cm^{-1} by the formation of Si–O–Ce bonds due to the large cation size difference[14] or it was also found in CeO_2–SiO_2–Al_2O_3 glass matrix.[15]

Ulbricht sphere photometers are used for diffuse reflection measurement. The resultant spectra can be used for characterization of the absorbance and band structure of the compound of interest. Fig. 5 shows reflection spectra of some synthesized powders with various Si/N substitution. These samples show strong absorption band in the blue region (420–500 nm), which is due to the lowest allowed $4f^1 \rightarrow 5d^1$ transitions of Ce^{3+}.[16] The resultant absorption of the blue light is efficiently downconverted into the yellow light.

The absorption edge on the reflection spectra corresponds to the position of the lowest energy absorption of the Ce^{3+} centres. It shows the green shift of the blue Ce^{3+} $4f^1 \rightarrow 5d^1$ absorption in powders with higher nitrogen substitution. Non-doped or low doped garnets show only one absorption edge at 530 nm corresponding to a band gap of 2.34 eV. The powders with higher nitrogen doping show two absorption edges at 510–515 nm (2.41–2.43 eV) and at 583–588 nm (2.11–2.14 eV). It is supposed that the first and second edges are related to the band structure of the Ce^{3+} centre, namely to the formation of additional Ce^{3+} centres that have N^{3-} ions in their nearest neighbour coordination, centres with lower energy. The newly formed N 2p band ($E_{2p}(O) = -14.8$ eV), which is located above the O 2p valence band ($E_{2p}(N) = -13.4$ eV) could be responsible for the low energy Ce^{3+} $4f^1 \rightarrow 5d^1$ absorption. Thus, crystal field splitting of the relevant lowest-energy level is modified by the electronegativity difference of the involved ions as Ce^{3+}–N^{3-} bonds show higher covalency versus oxygen bonded Ce^{3+}. The existence of the two absorption edges confirms earlier findings that only part of Ce–O bonds was replaced by the Ce–N ones.

Comparison between Si/N doped YAG:Ce samples shows a distinct change in splitting of Ce^{3+} $4f^1 \rightarrow 5d^1$ absorption energy between the low substituted garnets and those with higher nominal nitrogen content ($x = 0.6$). The former exhibits small distinctions between position of the lower energy Ce^{3+} centre and intensity. It is interesting to note that powders contaminated by $Y_2O_3 \cdot Si_3N_4$ (0.6-H) show the highest shift of lower energy Ce^{3+} centres. However, their absorption edge at lower wavelength below 400 nm is also modified, apart from lower absorption intensity. The reason is not very clear, however, there are some suggestions that oxygen vacancies could be responsible for such behaviour.[17]

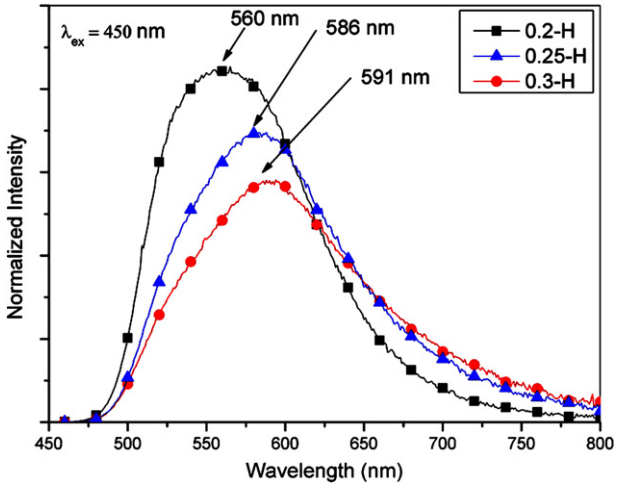

Fig. 6. Emission spectra ($\lambda_{exc.}$ = 450 nm) of (Si,N) doped YAG:Ce powders with nominal composition of $Y_{2.94}Ce_{0.06}Al_{(5-x)}Si_xO_{(12-x)}N_x$ for x = 0.2–0.3.

Fig. 6 shows the emission spectra of the Si,N doped garnets due to the electron transitions from the lowest crystal-splitting component of 5d level to the ground state Ce^{3+}. Both, intensity of the emission and the wavelength of the radiation are changed as a result of Si,N doping. The emission spectra present one broad emission band located from 450 to 800 nm. The wavelength maximum shift is noted from 560 nm (0.1-H) to 591 nm in the 0.3-H specimen. No additional wavelength shift was observed in specimens with nominal substitution over x = 0.3. The observed red shift is believed to be due to the existence of the two types of Ce^{3+} ions: higher energy sites with oxygen ligands and lower energy ones with partial substitution of Al–O for Si–N.

The red shift of emission is accompanied by simultaneous decrease of the fluorescence intensity and broadening of the emission band. If nominal substitution parameter x is over 0.2 then significant reduction of the emission intensity is observed. That finding is consistent with the phase composition of the N_2/H_2 derived specimens as increasing melilite precipitation could be responsible for the intensity drop. The highest red shift was noticed for 0.3-H specimens and formation of solid solution of Si,N in the YAG:Ce structure is confirmed. The obtained results show the new perspectives for further improvement of the synthesis techniques and application of Si,N doped YAG:Ce in a warm white LED.

4. Summary

The paper describes effects of formation of silicon nitride solid solution in yttria–alumina garnet doped with Ce by the means of the solid state reaction at 1650 °C. It has been found that the course of silicon/nitrogen YAG:Ce garnet doping as well as formation of the liquid phase and its chemical composition controlled formation of the side phase besides YAG:Ce. Precipitation of nitrogen melilite prevented higher substitution Al,O for Si,N in the garnet crystal lattice up to the nominal value of x = 0.3 in the compound with general formula of $Y_{2.94}Ce_{0.06}Al_{5-x}Si_xO_{12-x}N_x$. Formation of Si,N solid solution in the YAG structure with higher substitution degree, as evidenced by the parameters of the unit cell and FT-IR results, was possible but requires technological improvement. Nitrogen presence in the Ce^{3+} nearest coordination sphere altered the luminescence properties of the YAG:Ce garnet and a red shift of the emission maximum peak was observed.

References

1. Jang HI, Lee D, Jeon D, Kim. S. *J Luminesc* 2007;**126**(2):371–7.
2. Dorenbos P. *J Luminesc* 2002;**99**(3):283–99.
3. Li YQ, With G, Hintzen HT. *J Luminesc* 2006;**116**(1–2):107–16.
4. Sun WY, Li XT, Ma LT, Yen TS. *J Solid State Chem* 1984;**51**:315.
5. Setlur AA. *Chem Mater* 2008;**20**:2677–83.
6. Jack KH, Wilson WI. *Nat Phys Sci* 1972;**238**:28–39.
7. Kuru Y, Savasir O, Nergiz SZ, Oncel C, Gulgun MA, Haug S, et al. *J Am Ceram Soc* 2008;**91**(11):3663–7.
8. HSC Chemistry for Windows, Autokumpu, Finland, 1998.
9. Sopicka-Lizer M. *J Eur Ceram Soc* 2008;**28**:279–88.
10. Wu Z, Zhang X, He W, Du Y, Jia N, Xu G. *J Alloys Compd* 2009;**468**:571–4.
11. Zhou YH, Wang SB, Zhang HJ. *Opt Mater* 2002;**20**(1):13–20.
12. Fu YP. *J Alloys Compd* 2004;**414**:181–5.
13. Antsiferov VN, Gilyov VG, Karmanov VI. *Vib Spectrosc* 2002;**30**:169–73.
14. Kim BH, Selvaraj M, Lee TG. *J Appl Chem* 2005;**9**:316–9.
15. Lin SL, Shyang-Hwang C, Lee JF. *Mater Res Soc* 1996;**11**:2641–50.
16. Robbins DJ, Cockayne B, Glasper JL, Lent B. *J Electrochem Soc* 1979;**126**(7):1213–20.
17. Pankratov V, Shirmane L, Chudoba T, Gluchowski P, Hreniak D, Strek W, et al. *Radiat Measur* 2010;**45**(3–6):392–4.